CORPUS PUBLISHERS

Journal of Mineral and Material Science (JMMS)

ISSN: 2833-3616

Volume 7 Issue 3, 2026

Article Information

Received date : August 18, 2026

Published date: September 10, 2026

*Corresponding author

Hamdi Ekici, Ecole Supérieure de Gestion, Paris, France

DOI: 10.54026/JMMS/1140

Keywords

Shaft; Mandrel; Failure Analysis; Temper Mill; Fatigue; Microstructure; Predictive Maintenance

Distributed under Creative Commons CC-BY 4.0

Review Article

Damage Analysis Study of Temper Rolling Mill Mandrel Shaft

Onur Ay[1], Ali Cevahir Erkani[2], Hamdi Ekici[3*] and Bedirhan Güraydın[4]

[1,2,4]Trinox Metal San ve Tic AŞ, Tekirdağ, Turkiye

[3]Ecole Supérieure de Gestion, Paris, France

Abstract

Shafts are rotating mechanical elements, typically with a circular cross-section, used for transmitting motion and power in machinery while supporting components such as gears, belt-pulleys, or coupling hubs. These components may undergo sudden fractures due to improper material selection, exposure to excessive loads beyond design limits, completion of their service life, or various external factors. Such unforeseen failures lead to unplanned downtime in production lines, resulting in operational disruptions, as well as significant time and financial losses. Furthermore, these unexpected failures pose occupational health and safety risks, bringing along numerous unpredictable threats. Within the scope of this study, the fracture of a shaft used in a mandrel-the component responsible for rotating the rolls in a temper rolling mill-was investigated, and the root causes of the failure were comprehensively analyzed. The study involves a fracture surface analysis of the failed part, microstructural examinations, and destructive tests such as hardness, impact, and fatigue testing to understand material behavior. Based on the investigations, the service life of the shaft was determined in relation to its material properties, geometry, and operational conditions, followed by specific suggestions and recommendations to extend its service life.

Introduction

Stainless steels exhibit highly superior surface properties owing to their industrial corrosion resistance and aesthetic appearance. Particularly for flat-rolled stainless steels, low surface roughness customizes both custom and standard operational processes based on the specific application sector and field [1]. For cold-rolled stainless steels with 2B or BA surface finishes, the standard process steps involve cold rolling, followed by heat treatment and pickling for 2B finishes, or bright annealing in a protective atmosphere for BA finishes. Subsequently, steel sheets of both surface characters undergo temper rolling (skin pass milling) as the final process step, thereby transforming the flat-rolled cold-rolled stainless steels into finished products. Through temper rolling, Lüders bands in the material are eliminated, flatness is ensured, and ultimately, the 2B surface structure is obtained from the post-pickling 2D surface character while preserving BA surface properties. The roughness of the temper rolling mill rolls utilized for stainless steels is extremely low. Consequently, these low roughness values are transferred to the sheet through the pressure applied by the rolls, which reduces the material's roughness and yields a more homogenous surface finish [2].

Temper mills generally consist of an uncoiler mandrel, a recoiler mandrel, and housing sections accommodating the mill rolls. The uncoiler mandrel is positioned into the inner diameter of the coil, and the mandrel diameter is increased inside the coil to prevent it from rotating freely on the mandrel. Mandrels achieve this diameter expansion through the axial movement of the central expansion shaft, which radially pushes out the components referred to as mandrel segments. In the industry, this operation is called mandrel expansion. The technical drawings of the mandrel and the expansion shaft are illustrated in (Figure 1 & 2). The expansion shaft, designated as number 15 in the technical drawing, moves axially [3].

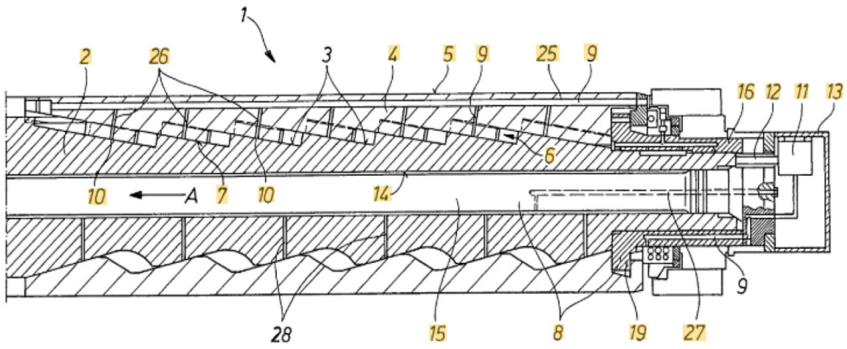

Figure 1: Cross-sectional view of a mandrel and its internal structure [3].

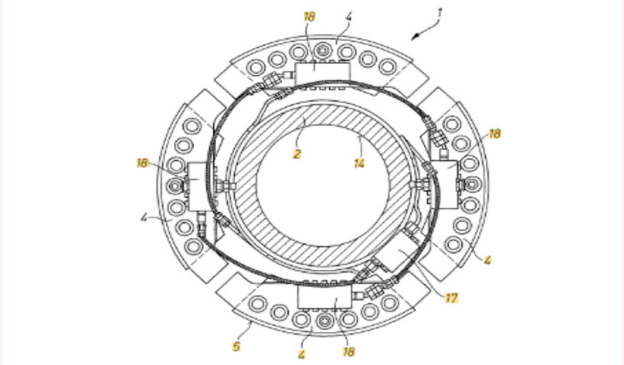

Figure 2: Vertical cross-sectional view of a mandrel [3].

The recoiler mandrel functions similarly to the uncoiler; the strip tip is engaged into the mandrel clamp, allowing the wraps to unwind from the uncoiler side, pass through the work rolls, and be wound on the recoiler side to form the final coil at the end of the passes. Reversible mandrels can operate as an uncoiler in one pass and act as a recoiler in the subsequent pass. Due to the weight of the coils, mandrels and their components are subjected to static loads, while the rotational effects subject them to dynamic loading. For these reasons, the operating loads and speeds must be well-defined during the design and utilization phases of the mandrels. While this status dictates critical inputs such as material selection and geometric configuration during the design stage, subjecting the existing equipment to loads beyond its design limits will lead to premature failures. Since they are the primary motion-generating systems in the process, failed or malfunctioning mandrels and their components can cause various levels of operational downtime in temper mills [4-6]. Mandrel failures within industrial machinery fleets can disrupt the entire production sequence, resulting in severe financial losses for enterprises.

Within the scope of this study, the temper mill utilized at the Trinox Metal cold rolling plant is a Tenova I2S SPM 2H 30”-50” brand and model. The root cause of the failure observed in the uncoiler mandrel expansion shaft of this mill-which can generate a tension force of 10.2 tons on both the uncoiler and recoiler sides, alongside a roll force of 1362 tons-has been investigated. The fractured expansion shaft has a total length of 4000 mm; a section of 3850 mm has a diameter of 100 mm, a section of 150 mm has a diameter of 75 mm, and a 71x3 thread is machined along a length of 120 mm. The thread root diameter is 68 mm with a thread angle of 60°. The technical drawing of the fractured shaft is illustrated in Figure 3. Within the scope of the investigation, the fracture surface failure analysis, material composition and microstructure analyses, and stresses under static and dynamic loading were examined. In light of the acquired data, design improvements and maintenance strategies are proposed to prevent recurring failures.

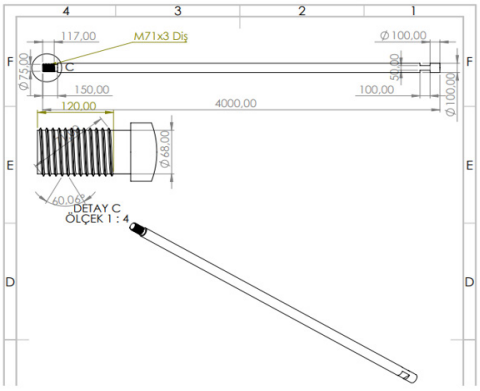

Figure 3: Technical drawing of the fractured component.

Fatigue in metallic materials

Fatigue in metals is a failure mechanism resulting from exposure to continuous and repetitive loads below the elastic limit of the material, which induces stress concentrations on the material surface or within its internal structure. Microscopic or macroscopic cracks on the material surface, inclusions, regional hardness variations, and phase discrepancies lead to the formation of slip bands in the material, thereby initiating the fatigue process [7]. The material undergoes three fundamental stages before experiencing fatigue-driven fracture. The first stage is micro-crack initiation. When the material is subjected to cyclic loading, stress concentrations develop in tandem with dislocation movements, and a micro-crack nucleates at the point where these concentrations reach their peak. The vast majority of the material’s fatigue life is consumed during this initial stage. Under the influence of ongoing cyclic loads, the micro-crack propagates and expands to a macroscopic level. Crack propagation traces become visible during this phase. This second stage, consisting of stable crack propagation, eventually gives way to the third stage: unstable crack propagation. In this final phase, the crack, which has propagated significantly and reduced the load-bearing cross-sectional area of the material, ultimately triggers ductile or brittle fracture depending on the material type, applied load, and number of cycles [8-10].

These stages can be observed in detail on fatigue-fractured surfaces. A crack initiated by an element creating a notch effect leaves fatigue striations behind as it propagates, ultimately reaching the critical threshold and culminating in fast fracture. Each of these stages can be thoroughly detailed on the fracture surface examined within the scope of this study [11,12]. To improve fatigue strength, elements that introduce discontinuities into the internal structure must be eliminated during the early stages of production. Intermetallic phases and incompatible phase regions are also microstructure-sourced factors that adversely affect fatigue resistance. Processes such as surface hardening and the induction of residual stresses enhance fatigue strength. Furthermore, final product attributes including design improvements, avoidance of sharp corners that induce notch effects, surface roughness, and tool maintenance during machining processes significantly influence overall fatigue performance [13,14].

Materials and Method

To determine the alloy composition and heat treatment condition of the fractured component under study, specimens were extracted from different sections of the expansion shaft to conduct spectral analysis, hardness mapping, and microstructural examination. In parallel with these investigations, the fracture surface was examined using a digital hand microscope at magnifications of 50X and 500X. A GNR S5 Solaris CCD Plus spectrometer was utilized for the chemical analysis. Hardness measurements were performed using an EmcoTest DuraScan 10 hardness tester, while macroscopic visual inspections were carried out with the aid of a digital hand microscope. For microstructural examinations, the specimens were mounted using the cold mounting method. The mounted samples were ground up to 1200 mesh using an ATM Qpol GO metallographic preparation unit, followed by polishing with diamond paste. After etching via the swabbing method using an aqua regia solution, the microstructures were examined using a Metkon metallographic microscope.

Results

Chemical composition and hardness analysis

The spectral analysis results obtained from the specimen extracted for the alloy identification of the fractured expansion shaft are presented in (Table 1). The resulting chemical composition indicates that the material corresponds to AISI/SAE 4140 (42CrMo4) steel [15]. To determine the heat treatment condition of the steel, a total of 60 hardness measurements were conducted across three different specimens taken from the shaft, along two distinct lines across the shaft diameter (Figure 4). The measurements revealed that the sections of the shaft defined as the head, middle, and end exhibited uniform hardness, with an average value of 280.13 HV. Furthermore, no hardness discrepancies were detected between the surface and the core of the shaft, indicating that no surface hardening treatment had been applied to this component. The acquired hardness value demonstrates that the material is a quenched and tempered 4140 alloy steel at its lower limit [15]. Additionally, the fact that specimens taken from different regions of the shaft display identical hardness values indicates the absence of any heat treatment defects. The microstructure images also support these findings.

For AISI 4140 steel, the range of 270-310 HV is the reference interval in the industry where the optimum balance of maximum ductility, impact toughness, and mechanical strength (the quenching and tempering quality) expected from shafts and spindles subjected to high dynamic loads is achieved [16]. This data demonstrates that the quenching and tempering (tempering) processes performed on the material were completed in accordance with the relevant standards [17-20].

Table 1: Table of chemical composition.

	%C	%Si	%Mn	%P	%S	%Cr	%Mo
Min.	0,38	0,15	0,5	0	0	0,9	0,15
Max.	0,45	0,4	0,8	0,035	0,035	1,2	0,3
Average of Measurement Results	0,401	0,210	0,725	0,018	0,019	0,983	0,163

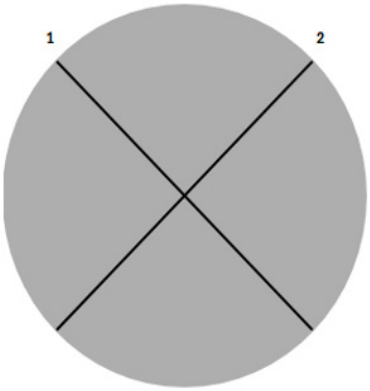

Figure 4: Schematic representation of the indentation zones for hardness measurements.

Metallographic examinations reveal that the microstructure generally exhibits an equiaxed and homogeneous morphology (Figure 5). No carbide precipitation along grain boundaries or formation of coarse ferrite structures is observed. In the micrographs, tempered martensite, obtained via the tempering process following the martensitic transformation during quenching, and partial regions of lower bainite phases can be identified. Furthermore, acicular martensite phases, which remain untransformed during heat treatment and impart brittleness to the material, are not encountered in the structure. This status demonstrates that the tempering heat treatment was performed correctly [21-22].

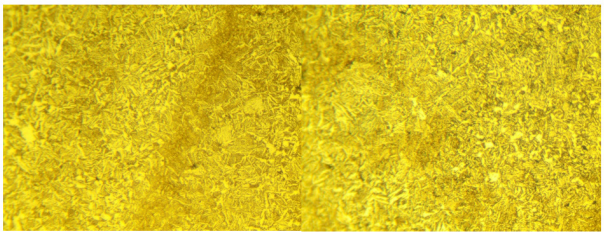

Figure 5: Microstructural images of the material.

Fracture surface analysis

The images regarding the fracture surface examinations are presented below in (Figure 6 & 7). When the fractured component is inspected, it is initially observed that the failure occurred at the root section of the screw thread machined onto the shaft. When the fracture surface is viewed from above, the fatigue propagation lines (beach marks) and the regions where unstable crack propagation took place are clearly visible. In the regions where the micro-crack nucleated and gave way to crack propagation, a flatter fracture surface resembling deformation-induced, relatively brittle fracture surfaces is observed; whereas in the unstable zone, the section that reached the critical diameter underwent a fully ductile fracture. The fracture surface exhibits characteristics typical of a fatigue-driven fracture surface [23].



Figure 6: Fracture surface micrographs of the shaft.

The thread crests and roots of the fractured component were among the specific locations subjected to detailed examination. Deformation and wear tracks were observed on the crest portions of the threads. Within the thread roots, machining-induced findings were encountered that formed surface notches, thereby increasing the roughness and laying the groundwork for micro-crack nucleation [24,25]. Performing the material removal process with blunted cutting tools may have generated surface deformations, consequently leading to the formation of residual stresses in these regions. No evidence of corrosion was encountered on either the fracture surfaces or within the thread roots. The absence of any corrosion findings indicates that the fatigue initiation was not corrosion-induced [26].

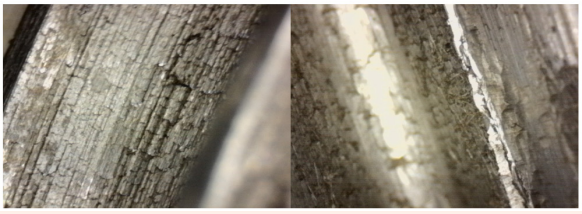

Figure 7: Detailed views of the fractured shaft thread roots.

Discussion

As a result of the elemental analysis, hardness mapping, and microstructural examinations, it was determined that the fractured expansion shaft was made of quenched and tempered 4140 steel. The hardness and microstructural outputs exhibited characteristics that provide optimal impact toughness, and no heat treatment-induced untransformed acicular martensite, carbide precipitation, or localized hardness variations were observed across different regions. Literature also supports that the material and heat treatment type selected in accordance with the design are highly suitable for shaft manufacturing. Fractographic examination of the failed region clearly demonstrated that the failure occurred due to a fatigue mechanism. Beyond this point, the aspect that requires further elaboration is the root cause of this fatigue initiation. Whether factors that increase the undetected vibration amplitude, to which the shaft and mandrel were exposed during dynamic loading, contributed to the damage remains a critical question [27]. Even if such an element inducing extra vibration on the mandrel existed, it was verified that the root sections of the screw threads machined on the fractured component possessed a notched and rough surface topography. Even when a machine element operates under ideal working conditions, the local stresses induced on the surface by a notched structure and the probability of micro-crack nucleation are among the primary factors that adversely affect fatigue resistance. Obtaining a surface finish of this nature indicates that the thread cutting process was executed either with a blunted tool or by rotating the workpiece at an excessively high cutting speed [28].

Conclusion

In this study, the unexpected fracture of an uncoiler mandrel expansion shaft utilized in a temper rolling mill was comprehensively investigated. Material analysis confirmed that the shaft was manufactured from appropriately quenched and tempered AISI 4140 steel, exhibiting an optimal hardness and a homogeneous microstructure free of heat-treatment defects. Fractographic analyses conclusively revealed that the

failure was driven by a fatigue mechanism originating at the root of the machined screw threads. The root cause of this fatigue initiation was identified as inadequate machining practices, which generated surface notches and excessive roughness that acted as critical stress concentrators for micro-crack nucleation [29-33].

Based on these findings and related literature, the following proactive measures and design improvements are strongly recommended to prevent recurrent failures and extend the service life of these shafts in production lines:

a) The mandrel must be regularly inspected to determine whether it is subjected to any non-axial (off-axis) loading.
b) The threaded section must be periodically tightened utilizing torque-controlled tools.
c) As an alternative to 4140 steel, an alloy with higher toughness and fatigue resistance, such as 4340, can be preferred.
d) Design inputs that induce notch effects within the thread roots can be rounded (filleted), thereby preventing potential design-sourced failures.
e) For machined components, it must be ensured that the workpiece is processed using sharp (non-blunted) cutting edges, correct rotational speeds, and optimal depths of cut. Post-machining surface roughness values must be minimized.
f) By applying a surface hardening treatment to the threaded section, the formation of wear-induced burrs on the thread crests can be prevented, and the toughness and fatigue strength of the treated portion of the component can be enhanced.

Acknowledgement

We would like to express our gratitude to the maintenance and quality technicians at Trinox Metal for their valuable assistance throughout this study.

References

1. Kijima H (2014) Influence of roll radius on roughness transfer in skin-pass rolling of steel strip. Journal of Materials Processing Technology 214(5): 1111-1119.
2. Özakin B, Kurgan N (2022) Investigation of the effect of rolling parameters in roughness transfer by skin-pass rolling to AISI 304 stainless steel sheet materials. Journal of Polytechnic 25(3): 1201-1209.
3. Patzelt U, Nosolik F (2008) Expandable and contractible coiler mandrel (U.S. Patent No. US7454937B2). U.S. Patentand Trademark Office.
4. Guo RM (2014) Cold rolling conditions using semi-analytic solutions of von Karman's rolling equation [Conference presentation]. International Conference on Rolling Mill Design, Tenova I2S, Yalesville, CT, United States.
5. Eldali A, Elghariani A, Elwaer S (2025) Reliability and performance analysis of cold rolling mill stands at LISCO.
6. Kao PW, Ho WY, Chang HC (2020) Premature failure analysis of mill rolls at China Steel Corp. China Steel Technical Report (36): 18-25.
7. Suresh S (1998) Fatigue of materials (2nd edn). Cambridge University Press, US.
8. Anderson TL (2017) Fracture mechanics: Fundamentals and applications (4th edn). CRC Press, US.
9. Pineau A, Weber B, Sudmanns M (2016) Fatigue of materials and structures: Introduction, initiation and propagation of cracks. International Journal of Fatigue 92: 461-467.
10. Ritchie RO (1999) Mechanisms of fatigue-crack propagation in ductile and brittle solids. International Journal of Fracture 100(1): 55-83.
11. Hull D (1999) Fractography: Observing, measuring and interpreting fracture surface topography. Cambridge University Press, US.
12. Schijve J (2009) Fatigue of structures and materials. (2nd edn). Springer Science & Business Media.
13. Stephens RI, Fatemi A, Stephens RR, Fuchs HO (2000) Metal fatigue in engineering (2nd edn). John Wiley & Sons.
14. Wohlfahrt H (1984) The influence of residual stresses on fatigue behavior. Residual Stresses 2: 85-116.
15. European Committee for Standardization (2006) Steels for quenching and tempering - Part 3: Technical delivery conditions for alloy steels (EN Standard No. EN 10083-3:2006).
16. Totten GE (Ed.), (2006) Steel heat treatment: Metallurgy and technologies (2nd edn). CRC Press, US.
17. ASM International. Handbook Committee (1991) ASM Handbook: Volume 4: Heat treating. ASM International.
18. Krauss G (2015) Steels: Processing, structure, and performance (2nd ed.). ASM International.
19. Lee WS, Su TT (1999) Mechanical properties and microstructural features of AISI 4140 high-strength alloy steel under dynamic loading. Journal of Materials Processing Technology 87(1-3): 198-206.
20. Smanio V, Fouvry S, Buffiere JY (2011) An experimental and numerical analysis of the microstructural mechanisms controlling fatigue crack initiation of quenched and tempered AISI 4140 steel. Materials Science and Engineering: A 528(19-20): 6103-6113.
21. Abdollah-Zadeh A, Salemi A, Assadi H (2008) Mechanical behavior of CrMo steel with tempered martensite and ferrite-bainite-martensite microstructure. Materials Science and Engineering: A 483-484: 325-328.
22. Krauss G (2005) Steels: Processing, structure, and performance. ASM International.
23. Bannantine JA, Comer JJ, Handrock JL (1990) Fundamentals of metal fatigue analysis. Prentice Hall, USA.
24. Javidi A, Rieger U, Eichlseder W (2008) The effect of machining on the surface integrity and fatigue life of AISI 4140 peerless steel. International Journal of Fatigue 30(10-11): 2050-2055.
25. Taylor D (2007) The theory of critical distances: A new perspective in fracture mechanics. Elsevier.
26. Jones DA (1996) Principles and prevention of corrosion (2nd edn). Prentice Hall, USA.
27. Rao JS (2011) Vibratory condition monitoring of machines. CRC Press, US.
28. Shaw MC (2005) Metal cutting principles (2nd ed.). Oxford University Press, England.
29. Bickford JH (2007) Introduction to the design and behavior of bolted joints: Non-gasketed joints (4th edn). CRC Press, USA.
30. Callister WD, Rethwisch DG (2020) Materials science and engineering: An introduction (10th edn). John Wiley & Sons.
31. Pilkey WD, Pilkey DF, Bi Z (2020) Peterson's stress concentration factors (4th edn). John Wiley & Sons.
32. Stephenson DA, Agapiou JS (2016) Metal cutting theory and practice (3rd edn). CRC Press, USA.
33. Davis JR (Ed.), (2002) Surface hardening of steels: Understanding the basics. ASM International.